2022

Changes in leaf anatomy of Betula papyrifera in response to elevated temperatures and atmospheric CO2 concentrations

Hailey Jaynes

Changes in leaf anatomy of *Betula papyrifera* in response to elevated temperatures and atmospheric CO_2 concentrations

Hailey Jaynes
Biology 4999E
Supervisor: Dr. Danielle Way
Mentor: Joshua Frank
Advisors: Dr. Hugh Henry & Dr. Natasha Mhatre
Friday, April 8th, 2022

ABSTRACT

As anthropogenic activity increases the concentration of atmospheric carbon dioxide ([CO_2]) and global temperatures, Canada's boreal tree species are at risk of reduced growth. The exchange of CO_2 and water between plants and the atmosphere is important for plant growth, as well as climate regulation. Leaves are the site of these exchanges, and therefore any structural changes in leaves due to environmental factors will impact these fluxes. Currently, there is little information available on the combined effects of elevated temperature and [CO_2] on leaf anatomy. This study examined changes in stomatal size and density, palisade layer length, overall leaf thickness, and length of spongy mesophyll exposed to intracellular air space in *Betula papyrifera* (white birch) under elevated temperature and [CO_2] as compared to ambient conditions. Plasticity among stomatal traits was observed in response to both temperature and [CO_2], with an overall increase in stomatal capacity at elevated temperatures to increase transpiration and facilitate evaporative cooling. Combined with reduced spongy mesophyll length, this suggests that there is a trade-off between leaf cooling and water retention via adjustment of internal and external leaf traits. Based on the results obtained in this study, temperature may be more a more important environmental factors in determining leaf anatomy than [CO_2]. Warming reduced palisade length at ambient [CO_2], but unexpectedly this effect disappeared with elevated [CO_2]. This is likely due to decreased efficiency in CO_2 uptake at ambient [CO_2] exacerbated by decreased spongy mesophyll cell length at elevated temperatures. Alternatively, there may be other factors at play, such as tradeoffs in leaf number, size and thickness based on carbon availability and temperature.

INTRODUCTION

Global Climate Change

For the past 10000 years, Earth's environment has been in a stable geological state known as the Holocene [1, 2]. However, since the dawn of the Industrial Revolution in 1790, Earth has undergone significant environmental transition. Human activity is a significant driver of global change, and has already pushed our planet away from the stable Holocene state, to the point where many researchers now recognize that we have entered a new geological period, the Anthropocene [1, 2]. A multitude of planetary boundaries have been proposed, beyond which Earth can no longer support our way of living. In 2009, it was suggested that [CO_2] not surpass 350 ppm, as the risk of irreversible climate change, including loss of major ice sheets, rapid shifts in forest systems, and accelerated rising sea levels, would drastically increase [1]. Unfortunately, we have already passed this boundary, as our current [CO_2] sits at 415.61 ppm [3].

Measurements of [CO_2] have been made continuously since 1957 [4], documenting increases in tropospheric [CO_2], as well as seasonal cycles due to terrestrial ecosystem activity in the Northern Hemisphere [3, 4]. These measurements, in conjunction with ice-core records, have allowed us to determine that the aforementioned increase in [CO_2] is unprecedented when compared with previous natural fluctuations [3, 4]. According to the National Oceanic and Atmospheric Administration, global [CO_2] has risen by 80 ppm since 1980 [3]. This has led to an increase of global surface temperatures by 0.18°C per decade [3], a rate far greater than any preceding decade [1, 2, 4]. Without the implementation of mitigation strategies and climate policies, this trend will continue. Based on the RCP 8.5 climate scenario proposed by the Intergovernmental Panel on Climate Change [Fig. 1], by the year 2100, Earth could see [CO_2] of

1200 ppm [5]. This would cause mean global temperature increases of 4.3°C, which would increase mean boreal temperatures by ~8°C [5, 6].

Leaf Anatomy and Elevated [CO_2] and Temperature

Stomata are small pores on the leaf surface that regulate the exchange of CO_2 and water between plants and the atmosphere. The size of the stomatal pore determines the rate of gas diffusion through the pore, with the opening and closing of the stomata controlled by guard cells, which form the pore [7, 8]. When the stomata are open, CO_2 diffuses into the leaf while O_2 and water diffuse out, such that plants must balance the intake of CO_2 for photosynthesis with water loss to the atmosphere [7]. Thus, changes in the environment that affect photosynthesis and/or water availability, such as humidity, light intensity, and [CO_2], trigger signalling cascades that cause stomata to open and close [8], or change their size and density during leaf development.

Under elevated [CO_2], the CO_2 concentration gradient between the atmosphere and leaf interior is steeper, meaning CO_2 diffuses more easily into the leaf [8]. As such, trees grown at high [CO_2] typically have reduced stomatal conductance and transpiration, and increased water-use efficiency [7, 9]. With increased [CO_2], most leaves develop smaller stomata and fewer stomata per leaf unit area (stomatal density) [7, 8, 9]. Reduced stomatal density in plants grown under elevated [CO_2] has also been attributed to a notable increase in leaf area [7] and down-regulation of genes associated with stomatal development [7, 8].

Stomatal traits (size and density) also decrease with increasing temperature [9], as a means to prevent excess water loss due to the higher vapour pressure deficit (the difference between the amount of moisture in the air and the maximum potential moisture at saturation) associated with warmer air [10, 11, 12]. Transpiration is lower in leaves with reduced stomatal traits, which restricts the diffusion of water out of leaves [10, 11]. However, reduced stomatal traits also limit latent cooling [13], which implies that plants prioritize water retention may be more susceptible to heat stress.

Mesophyll tissues are found within dicotyledonous leaves are composed of two types od cells: palisade mesophyll cells and spongy mesophyll cells [14]. Palisade cells are the primary location of photosynthesis. They contain 70% of all chloroplasts in the leaf [14] and are tightly packed near the upper leaf (adaxial) surface to maximize light absorption [Fig. 2]. Spongy mesophyll cells are located below the palisade cells, closer the the lower (abaxial) leas surface, and are round and loosely packed [Fig. 2]. Although spongy mesophyll cells contain some chloroplasts, these cells are located far below the leaf surface, limiting light absorption to high intensities [14]. Instead, spongy mesophyll cells function to facilitate the gas and water exchange necessary for photosynthesis.

Though there has been extensive research conducted regarding response of leaf traits to elevated temperature and [CO_2] individually, there has been limited investigation into the combined effects of these environmental stimuli.

Boreal Forests

Global warming is not uniform across the planet [6]; high latitude regions, which include boreal forests, are predicted to warm by more than 8°C throughout the next 80 years [5] — a faster rate of warming than expected for most regions. Boreal regions account for 30% of the world's forests, making them an important ecosystem for CO_2 exchange with the atmosphere.

Further, boreal forests engage in many complex feedback loops with climate systems, including precipitation and fires, such that tree responses to elevated temperatures and [CO_2] can either accelerate or slow global change [15]. Therefore, it is critical to understand the anatomical and physiological responses of boreal trees to climate change so that their future CO_2 exchange can be accurately modelled. Determining the mechanisms underlying tree responses to elevated temperature and [CO_2] will provide insight into ecosystem changes with respect to climate [15].

Betula papyrifera (Marshall), or white birch, is a broad-leaf deciduous tree known for its striking white, paper-like bark. This tree has a wide range across North America [Fig. 3]. White birch is a pioneer species, colonizing communities in disturbed areas, which makes it a dominant member of boreal ecosystems where fire return intervals are frequent [16]. Understanding leaf anatomical responses of white birch to elevated [CO_2] and temperature is important in determining how plant CO_2 and water fluxes will change with the climate. Given its range and abundance, studying white birch leaf anatomy could provide insights into the CO_2 storage capacity of the North American region as a whole [15].

OBJECTIVE, HYPOTHESES, AND PREDICTIONS

The objective of my research project was to examine the impacts of elevated temperatures and [CO_2] on the internal and external leaf anatomy of *B. papyrifera*. I hypothesize that white birch will adjust its stomatal traits and mesophyll tissue morphology to maximize carbon gain and minimize water loss and heat stress when grown under high [CO_2] and warming conditions. I predict that plants grown under elevated [CO_2] will produce thicker leaves with longer palisade mesophyll cells [17] and reduced stomatal traits (size and density). At increased temperatures, I expect to see a thinner leaves [18] due to cellular heat stress, and a further reduction of stomatal traits. Under combined elevated temperatures and [CO_2], I predict that stomatal traits will be lower than in either high [CO_2] or warm-grown plants independently, but that leaves will not differ in thickness compared to those grown under ambient [CO_2] and temperatures. As for spongy mesophyll cells, I predict that cell length exposed to intracellular air space will increase under future climate change conditions due to an increased demand for gas exchange and water-use efficiency [19].

METHODS AND MATERIALS

Plant Material and Experimental Growth Conditions

Betula papyrifera (Marshall) was grown from seed at Western University's Biotron Experimental Climate Change Research Centre (43.0096ºN, 81.2737ºW) in early May 2021 by the Way lab. Seeds were sourced from between 45-46ºN in Ontario (near the southern range of the species) and sown in 11.6 L pots filled with Pro-Mix BX Mycorrhizal growth medium (Premier Tech Home and Garden, QC, Canada) and slow-release fertilizer (Slow-Release Plant Food, 12-4-8, Miracle Gro®, The Scotts Company, Mississauga, ON, Canada).

Six glasshouses were set to six factorial climate treatments: ambient (AC, 410 ppm) or elevated [CO_2] (EC, 750 ppm) with either ambient temperature (T0), or +4°C (T4) or +8°C (T8) warming to simulate moderate and extreme climate scenarios [Table 1]. The ambient temperatures follow a five-year day/night average for Algonquin Park, ON (45º58'N, 78º48'W) to align with the climate at the seed source. Pure CO_2 was added to the air as needed to maintain EC levels. Relative humidity was kept above 60%.

There were 6 pots per treatment (total N=36). Watering was provided as needed to prevent water stress, and soil moisture was checked for consistency among treatments using a soil moisture probe (HH2 Moisture Meter, Delta-T Devices, Cambridge, UK). Seedlings were grown for 6 months (October 2021) before leaves were harvested for measuring stomatal traits and internal anatomy.

Stomatal Traits

For each climatic condition, six mature leaves per treatment were collected and used to obtain a negative mould of the leaf surface following Duarte et al. [20]. Dental resin (President SEM High Resolution Replication Kit, TED Pella Inc.) was spread on a 3 cm × 1 cm area on the abaxial surface of each leaf. A positive mould was then obtained by applying a layer of wet clear nail varnish to the negative mould. Once dry, the layer of nail polish was then carefully removed and fixed to a microscope slide. Using the positive mould, stomatal traits were assessed and imaged at a magnification of 20× magnification using a Zeiss Lumar.V12 Stereoscope.

Leaf Thickness and Mesophyll Characteristics

A subsample of leaves was harvested for microscope analysis of mesophyll traits from six seedlings per climate condition. Strips of tissue were taken from fresh leaves from a uniform location across the full width of the leaf and washed with de-ionized water. Leaf tissues were stored in buffered 2% paraformaldehyde with 0.1% Triton X-100 and placed in a vacuum chamber overnight to force the solution into the leaf air spaces. Excess solution was drawn off the next day, and samples were rinsed in Microtubule-Stabilizing Buffer under vacuum three times over 24 hours. Following this, samples were rolled up and placed into tissue cassettes in 70% ethanol. Leaf tissues were then transferred to an external lab for processing and paraffinization.

Semi-thin sections (1.0 μm) were cut using a razor blade, and fixed on a microscope slide. The slides were then deparaffinized in decreasing concentrations of xylene and ethanol, and stained with 0.02% Calcofluor White to visualize the internal leaf structures. Photographs of stained sections were taken with a Zeiss Lumar.V12 Stereoscope.

Data Collection and Statistical Analyses

When assessing both internal and external leaf anatomy, ImageJ software was used to define areas, and count and measure various traits.

For stomatal density, an area of 2500 μm^2 was randomly selected for each leaf, and the number of stomata in this area was counted [Table 2]. Stomatal density was then calculated as:

Stomatal density = number of stomata/unit area

In each of the six conditions, for each of which there were six leaves, 10 stomata were selected from the same area, and their length was measured, totalling 60 measurements for each condition [Table 3]. The mean value for each leaf was used for data analysis.

The cross-sectional palisade layer length [Table 4] and leaf thickness [Table 5] were measured at randomly selected locations along the leaf with 10 measurements taken for each leaf, totalling 60 measurements for each condition. The mean value for each leaf was used for data analysis.

An 100 μm wide area was randomly selected for each leaf cross-section. The length of spongy mesophyll exposed to intracellular air space was then measured. Each leaf was measured 10 times at randomly selected locations, resulting in a total of 60 measurements for each condition [Table 6]. The mean value for each leaf was used for data analysis.

Data exploration and statistical analyses were performed using GraphPad software by Prism. Two-way ANOVAs were used to analyze the effects of growth temperature, growth [CO_2] and their interaction on leaf traits (stomatal size, stomatal density, leaf thickness, palisade mesophyll cell layer length, and spongy mesophyll cell length exposed to intracellular air space). A post-hoc Tukey test was used when signifiant treatment effects were found. All data are reported as means ± standard errors.

RESULTS

Stomatal Size and Density

Both temperature, [CO_2], and the interaction between the two variables influenced stomatal density [Fig. 4]. Warming increased stomatal density ($F=158.7$, $P<0.0001$), with a 20% increase from T0 to T8 in AC leaves and a 30% increase from T0 to T8 in EC leaves [Fig. 4]. However, elevated [CO_2] reduced ($F=83.24$, $P<0.0001$) stomatal density [Fig. 4]. When comparing AC to EC, stomatal density decreased by 25% in T0, 5% in T4, and 3% in T8 [Fig. 4]. The significant interaction between temperature and [CO_2] ($F=29.42$, $P<0.0001$) [Fig. 4] describes this reduced [CO_2] effect with warming. When comparing current (ACT0) to future (ECT8) climate conditions, there was an overall 8% increase in stomatal density [Fig. 4].

Though there was no significant [CO_2] or interaction effects, warming reduced stomatal size ($F=32.95$, $P<0.0001$) [Fig. 5]. Stomata were 15% smaller in ACT8 leaves compared to ACT0 leaves, and 10% smaller in ECT8 leaves compared to ECT0 leaves [Fig. 5]. When comparing current (ACT0) to future (ECT8) climate conditions, there was an overall 13% decrease in stomatal size [Fig. 5].

Palisade Layer Length and Leaf Thickness

Neither temperature nor [CO_2] had an impact on palisade layer length independently, but there was a significant interaction effect ($F=5.908$, $P=0.0069$) [Fig. 6]. At T0, elevated [CO_2] decreased palisade layer length, but at T4 and T8, elevated [CO_2] increased palisade layer length [Fig. 6]. In AC leaves, palisade layer length decreased by 14% from T0 to T8, whereas in EC leaves, palisade layer length increased by 19% from T0 to T8 [Fig. 6].

There were no significant differences in leaf thickness among the different climate treatments [Fig. 7].

Length of Spongy Mesophyll Exposed to Intracellular Air Space

No significant differences were observed for the length of spongy mesophyll exposed to intracellular air space for [CO_2] independently or in combination with warming [Fig. 8]. As an independent factor, warming significantly decreased ($F=8.506$, $P=0.0012$) spongy mesophyll length exposed to intracellular air space, with a 17% decrease from T0 to T8 in AC leaves and 14% decrease from T0 to T8 in EC leaves [Fig. 8]

DISCUSSION

Plasticity Among Stomatal Traits for Evaporative Cooling

Both stomatal size and stomatal density influence CO_2 uptake, water loss, and leaf cooling. Stomatal density represents the number of sites available for gas and water exchange, whereas stomatal size represents the available area for this exchange at each site. Thus, it is important that these traits be examined together. In AC, warming increased stomatal density by 20%, but reduced stomatal size by 15% [Fig. 4, Fig. 5]. Taken together, the stomatal capacity, or the ability for the stomata to carry out exchange of water and gases, increased by 5% at elevated temperatures [Fig. 4, Fig. 5]. In EC, warming increased stomatal density by 30% and decreased stomatal size by 10%, resulting in an overall 20% increase in stomatal capacity [Fig.4, Fig. 5]. These results suggest that with increasing temperature, leaves are increasing transpiration rates in effort to decrease leaf temperature through evaporative cooling [22, 23]. However, increased rates of transpiration can lead to water loss, especially when warming increased the vapour pressure deficit (drying) of the air, so leaves most conserve water in other ways.

Interestingly, warming generally increases stomatal capacity. However, EC leaves increase stomatal capacity (20%) more than their AC counterparts (5%). A decrease in stomatal density at elevated [CO_2] is considered to be a common response [7]. Therefore, as reflected in the results, ECT0 leaves have a lower stomatal density than ACT0 leaves, by 22% [Fig. 4]. Consequently, there is a greater increase of stomatal density from ECT0 leaves to ECT8 leaves compared to ACT0 leaves to ACT8 leaves [Fig. 4] to compensate for heat stress.

Internal Management of Water Loss

The increase stomatal capacity as a means for evaporative cooling under warm conditions increases the risk of water loss. However, trees grown under elevated temperatures also decreased the length of spongy mesophyll cells exposed to intracellular air space [Fig. 8]. This provides a possible explanation for why warmed trees increased their stomatal capacity at the risk of becoming water stressed. Before water is transpired by the leaf through its stomata, it must first evaporate from the leaf tissues into the intracellular air space. By reducing spongy mesophyll cell length, leaves limit the cell surface area exposed to the intracellular air space and thereby minimize water evaporation from these surface. Therefore, although there was an increase in stomatal capacity and potential transpiration in warm-grown leaves [Fig. 4, Fig. 5], water stress can be mitigated internally [Fig. 8]. This allows for a balance to be maintained between leaf temperature and the rate of water loss.

The increase in stomatal capacity is greater than the reduction in the length of spongy mesophyll exposed to intracellular air space [Fig. 4, Fig. 5, Fig. 8], which suggests that leaf cooling is more important than reducing water loss under warming. However, it is important to note that seedlings were grown in well-watered pots, and therefore may not have experienced the degree of water stress that might occur in their natural environment. With warming expected to continue in the future, boreal will face increased atmospheric drying and water loss. This could have large-scale impact on tree growth, possibly even leading to tree mortality [25] which will in turn increase the frequency and scale of fire disturbances [26]. White birch is known to be a pioneer species, particularly after fire intervals [16], so it is possible that it may become a dominant species in the North American boreal forest as climate change progresses.

Importantly, by reducing the cell surface area available for water exchange, the rate of CO_2 uptake is also limited. This implies that photosynthesis is reduced. Thus, at elevated temperatures, the leaf thickness and length of palisade layer should decrease as a result of reduced CO_2 availability.

Suppression of Palisade Layer Thickness at Ambient CO_2 Conditions

At ambient [CO_2] conditions, warming suppressed the palisade layer length [Fig. 6], but at elevated [CO_2], this effect disappeared and the length was approximately constant across all temperature treatments [Fig. 6].

Increasing temperature can have negative effects on leaf structure and function [24], resulting in thinner leaves and lower rates of photosynthesis. Therefore, the reduction of palisade layer length with warming at ambient [CO_2] is not surprising. However, this same effect is not observed at elevated [CO_2]. The observed reduction in length of spongy mesophyll with warming could explain these results. The warming-induced reduction in surface area for gas exchanged reduced the ability of trees to facilitate CO_2 uptake. Under ambient [CO_2], carbon is less readily available in the atmosphere. This limits CO_2 uptake efficiency, causing decreased rates of photosynthesis [24]. However, elevated [CO_2] increases the availability of carbon in leaf tissues allowing for greater photosynthetic rates. Therefore, the reduction of spongy mesophyll cell length exposed to intracellular air space can limit CO_2 uptake, but only when atmospheric CO_2 is not readily available.

Overall, there is little difference in palisade layer length between ACT0 and ECT8, as predicted. Elevated temperatures place stress on leaf physiology resulting in reduced CO_2 uptake and shorter palisade layers, but this effect disappears when [CO_2] is high. As a result, there was no significant difference between current and future climate conditions with respect to palisade layer length. These results suggest that climate change may not directly impact the growth of white birch and other boreal trees. However, this study only used seedlings, not mature trees, and these changes in leaf anatomy could be highly-dependent on the conditions under which the leaves develop. Therefore, we might see variation in leaf anatomy from year to year as new leaves grow in the spring, which could have a cumulative effect on overall tree growth and performance. Coniferous tree growth is likely less dependent on annual conditions than deciduous trees, such as white birch, so it is possible that there will be a shift in species dominance.

Alternatively, it is possible that the observed reduction in palisade layer length is not the result of reduced CO_2 uptake, but instead simply due to a variation in carbon investment at ambient temperatures. For instance, warming may pressure trees to produce fewer thicker leaves, whereas at ambient temperatures trees might yield more thinner leaves.

CONCLUSION

In investigating the plasticity of leaf traits in response to rising [CO_2] and temperatures, assumptions about the physiological responses of boreal tree species to climate change can be made. While temperature and [CO_2] have significant impacts on stomatal density, resulting in an overall increase, temperature simultaneously reduces stomatal size. The combined effect of these changes in leaf traits resulted in an overall increase in stomatal capacity, suggesting *B. papyrifera* prioritizes evaporative cooling at elevated temperatures. However, increased transpiration poses the risk of severe water loss, especially as warming dries the air and soil. *Betula papyrifera* may manage this by reducing the length of spongy mesophyll exposed to intracellular air space, which is the site of water evaporation. Thus, it is possible that there is an elegant tradeoff between leaf cooling and water retention via changes in internal and external leaf anatomy. Warming suppresses palisade layer thickness at ambient [CO_2], but this effect is not observed at elevated [CO_2]. It is possible that there is a tradeoff in investment of carbon between leaf thickness and number based on temperature. Overall, we can expect boreal tree species that experience heat stress with future climate change to adjust their internal and external leaf anatomy to promote leaf cooling while preventing excess water loss, although likely at the expense of CO_2 uptake.

ACKNOWLEDGEMENTS

I would like to thank my supervisor, Dr. Danielle Way, and my mentor, Joshua Frank, for providing me with incredible guidance and direction throughout the completion of this project. I would also to thank Dr. Natasha Mhatre and Dr. Hugh Henry for their feedback and support as my advisors. I would also like to thank the Biotron Staff; Kyle Doward for his assistance in lab coordination, Marc Courchesne for his experience is tissue sectioning, and Karen Nygard for her critical support in developing my microscopy skills. Further, I thank Julia Hammer for providing me with detailed information regarding seeding growth methods and for her invaluable mentorship in data analysis. Finally, I am appreciative of and thank the Way Lab as a whole; Kiana Lee, Andrew Cook, Samuel Woolsey, and Robyn Swartman, for their critical feedback, review and support of my thesis.

REFERENCES

1. Rockström J, Steffen W, Noone K, Persson Å, Chapin FS III, Lambin EF. A safe operating space for humanity. Nature. 2009;461(24):472-475. doi: 10.1038/461472a.

2. Steffen W. The Anthropocene, global change, and sleeping giants: where on Earth are we going? Carbon Balance Manag. 2006;1(1):3. doi: 10.1186/1750-0680-1-3.

3. NOAA [Internet]. Trends in atmospheric carbon dioxide. National Oceanic and Atmospheric Administration. c2021 [cited 2021 Oct 10]. Available from: https://gml.noaa.gov/ccgg/trends/

4. Vitousek PM. Beyond global warming: ecology and global change. Ecology. 1994;75(7):1861-1876. doi: 10.2307/1941591.

5. Stocker TF, Qin D, Plattner G, Tignor M, Allen SK, Boschung J, Nauels A, Xia Y, Bex V, Midgley PM. Climate Change 2013: The Physical Science Basis. Contribution of Working Group I to the Fifth Assessment Report of the Intergovernmental Panel on Climate Change. Cambridge, United Kingdom and New York, NY, USA: Cambridge University Press; 2013 Sep. ISBN: 978-92-9169-138-8.

6. Ruiz-Pérez G, Vico G. Effects of temperature and water availability on northern European boreal forests. Front For Glob Change. 2020;3. doi: 10.3389/ffgc.2020.00034.

7. Xu Z, Jiang Y, Jia B, Zhou G. Elevated-CO_2 response of stomata and its dependence on environmental factors. Front Plant Sci. 2016;7:657. doi: 10.3389/fpls.2016.00657.

8. Ainsworth EA, Rogers A. The response of photosynthesis and stomatal conductance to rising [CO_2]: mechanisms and environmental interactions. Plant Cell Environ. 2007;30:258-270. doi: 10.1111/j.1365-3040.2007.01641.x.

9. Zheng Y, Li F, Has L, Yu J, Guo L, Zhou H, Ma C, Zhang X, Xu M. Elevated CO_2 concentration induces photosynthetic down-regulation with changes in leaf structure, non-structural carbohydrates and nitrogen content of soybean. BMC Plant Biol. 2019;19:255. doi: 10.1186/s12870-019-1788-9.

10. Zhao J, Hartmann H, Trumbore S, Ziegler W, Zhang Y. High temperature causes negative whole-plant carbon balance under mild drought. New Phytol. 2013;200(2):330-339. doi: 10.1111/nph.12400.

11. Kirschbaum MUF, McMillian AMS. Warming and elevated CO_2 have opposing influences on transpiration: which is more important? Curr Forestry Rep. 2018;4(2):51-71. doi: 10.1007/s40725-018-0073-8.

12. Hasper TB, Wallin G, Lamba S, Hall M, Jaramillo F, Laudon H, Linder S, Medhurst JL, Räntfors M, Sigurdsson BD, Uddling J. Water use by Swedish boreal forests in a changing climate. Funct Ecol. 2015;30(5):690-699. doi: 10.1111/1365-2435.12546.

13. Leaky ADB. Rising atmospheric carbon dioxide concentration and the future of C_4 crops for food and fuel. Proc Biol Sci. 2009; 276(1666):2333-2343. doi: 10.1098/rspb.2008.1517.

14. Gotoh E, Suetsugu N, Higa T, Matsushita T, Tsukaya H, Wada M. Palisade cell shape affects the light-induced chloroplast movements and leaf photosynthesis. Sci Rep. 2018;8(1):1472-1479. doi: 10.1038/s41598-018-19896-9.

15. Hyvönen R, Ågren GI, Linder S, Persson T, Cotrufo MF, Ekblad A, Freeman M, Grelle A, Janssens IA, Jarvis PG, Kellomäki S, Lindroth A, Loustau D, Lundmark T, Norby RJ, Oren R, Pilegaard K, Ryan MG, Sigurdsson BD, Strömgren M, Van Oijen M, Wallin G. The likely impact of elevated [CO_2], nitrogen deposition, increased temperature and management on carbon sequestration in temperate and boreal forest ecosystems: a literature review. New Phytol. 2006;173:463-480. doi: 10.1111/j.1469-8137.2007.01967.x.

16. USDA [Internet]. Index of species information: *Betula papyrifera*. United States Department of Agriculture. c2021 [cited 2021 Oct 7]. Available from: https://www.fs.fed.us/database/feis/plants/tree/betpap/all.html

17. Way DA. Tree phenology responses to warming: spring forward, fall back? Tree Physiol. 2011;31(5):469-471. doi: 10.1093/treephys/tpr044.

18. Way DA, Oren R, Kim H, Katul GG. How well do stomatal conductance models perform on closing carbon budgets? A test using seedlings under current and elevated air temperatures. J Geophys Res Biogeosci. 2011;116(G4). doi: 10.1029/2011JG001808.

19. Nelson EA, Sage TL, Sage RF. Functional leaf anatomy of plants with crassulacean acid metabolism. Funct Plant Biol. 2005;32(5):409-419. doi: 10.1071/FP04195.

20. Duarte AG, Longstaff FJ, Way DA. Nitrogen fertilization influences low CO_2 effects on plant performance. Funct Plant Biol. 2020;47(2):134-144. doi: 10.1071/FP19151.

21. Liu Y, Li X, Chen G, Li M, Liu M, Liu D, Li M. Epidermal micromorphology and mesophyll structure of *Populus euphratica* heteromorphic leaves at different development stages. PLoS One. 2015;10(9):e137701. doi: 10.1371/journal.pone.0137701.

22. Hill KE, Guerin GR, Hill RS, Watling JR. Temperature influence stomatal density and maximum potential water loss through stomata of *Dodonaea viscosa* subsp. *angustissima*

along a latitude gradient in southern Australia. Aust J Bot. 2015;62(8):657-665. doi: 10.1071/BT14204.

23. Wu G, Liu H, Hua L, Lou Q, Lin Y, He P, Feng S, Liu J, Ye Q. Differential responses of stomata and photosynthesis to elevated temperature in two co-occurring subtropical forest species. Front Plant Sci. 2018;9:467. doi: 10.3389/fpls.2018.00467.

24. Thompson M, Gamage D, Hirotsu N, Martin A, Seneweera A. Effects of elevated carbon dioxide on photosynthesis and carbon portioning: a perspective on root sugar sensing and hormonal crosstalk. Front Physiol. 2017;8. doi: 10.3389/fphys.2017.00578.

25. Murphy BK, Way DA. Warming and elevated CO_2 alter tamarack C fluxes, growth and mortality: evidence for heat-stress related C starvation in the absence of water stress. Tree Physiol. 2021:41(12):2341-2358. doi: 10.1093/treephys/tpab077.

26. Sulla-Menashe D, Woodcock CE, Friedl MA. Canadian boreal forest greening and browning trends: an analysis of biogeographic patterns and the relative roles of disturbance versus climate drivers. Environ Res Lett. 2018;13:014007. doi: 10.1088/1748-9326/aa9b88.

FIGURES AND TABLES

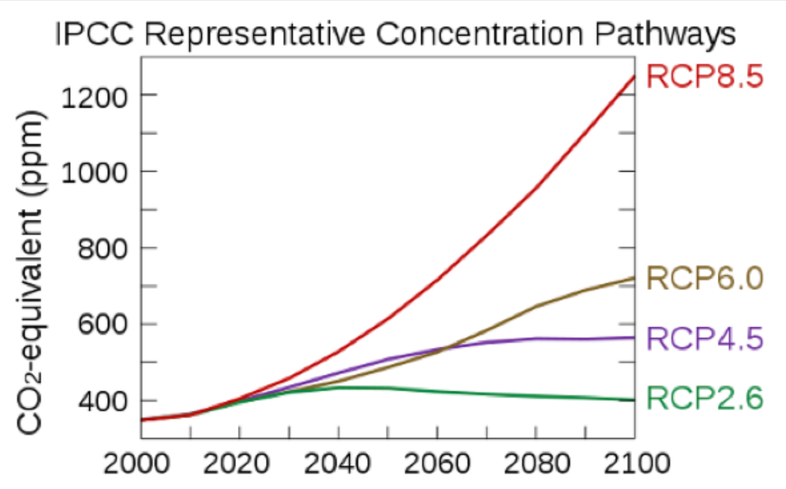

Figure 1. Predicted future climatic outcomes as denoted by [CO_2], varying by mitigation strategy. Obtained from Stocker et al., 2013 [5].

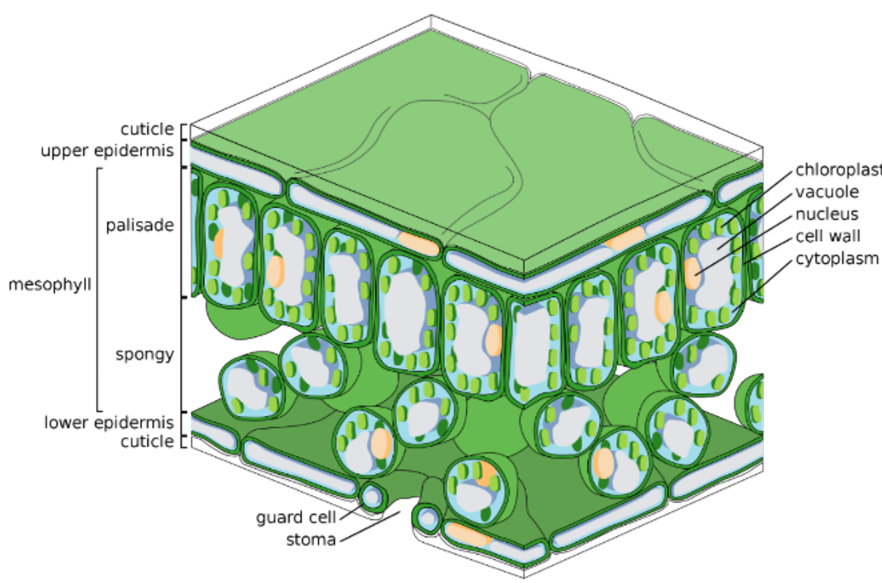

Figure 2. Cross-sectional internal leaf anatomy.Demonstrates differences in shape and distribution of palisade mesophyll and spongy mesophyll. Obtained from: https://www.microscopemaster.com/mesophyll-cells.html#gallery[pagegallery]/1/

Figure 3. Range map of Betula papyrifera, or white birch tree. Areas highlighted in green represent the locations where the species grows naturally. Obtained from USDA, 2021 [16].

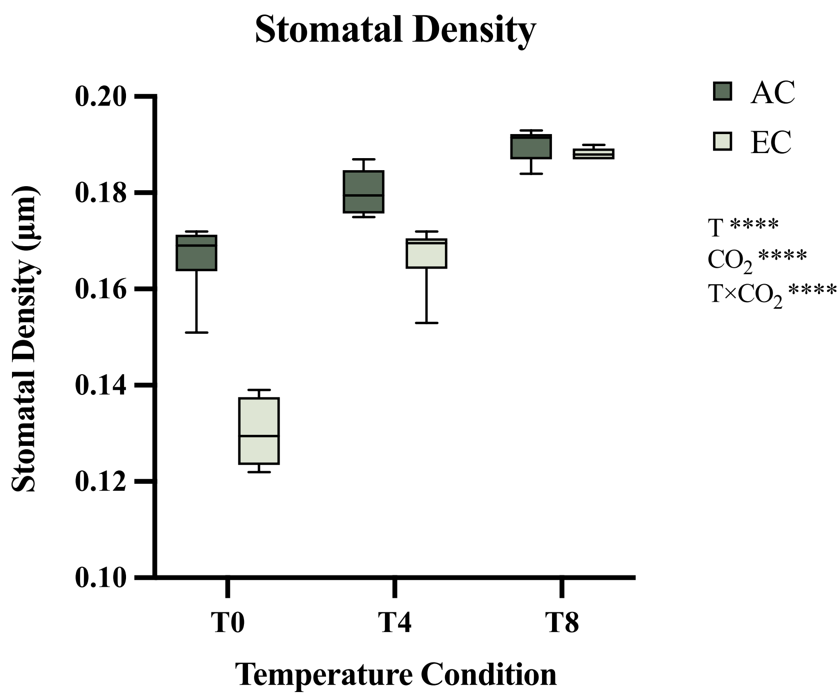

Figure 4. Mean (± SE) stomatal density of *Betula papyrifera* at various climate conditions, where AC represents ambient atmospheric [CO_2] at 410 ppm, EC represents elevated atmospheric [CO_2] at 750 ppm, T0 represents ambient temperature, T4 represents +4°C warming, and T8 represents +8°C warming.

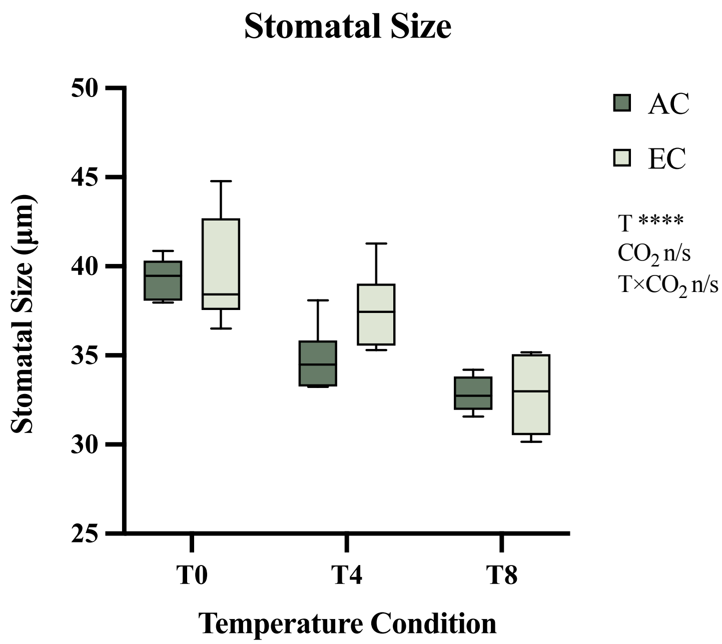

Figure 5. Mean (± SE) stomatal size of *Betula papyrifera* at various climate conditions, where AC represents ambient atmospheric [CO_2] at 410 ppm, EC represents elevated atmospheric [CO_2] at 750 ppm, T0 represents ambient temperature, T4 represents +4°C warming, and T8 represents +8°C warming.

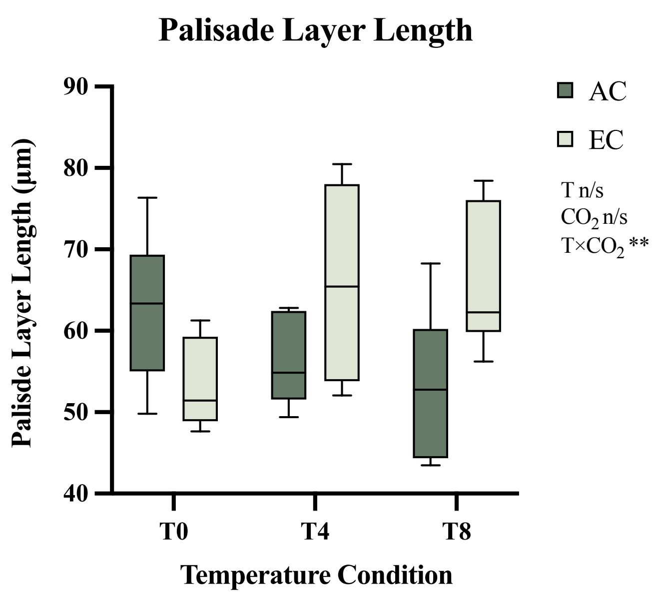

Figure 6. Mean (± SE) palisade layer length of *Betula papyrifera* at various climate conditions, where AC represents ambient atmospheric [CO_2] at 410 ppm, EC represents elevated atmospheric [CO_2] at 750 ppm, T0 represents ambient temperature, T4 represents +4°C warming, and T8 represents +8°C warming.

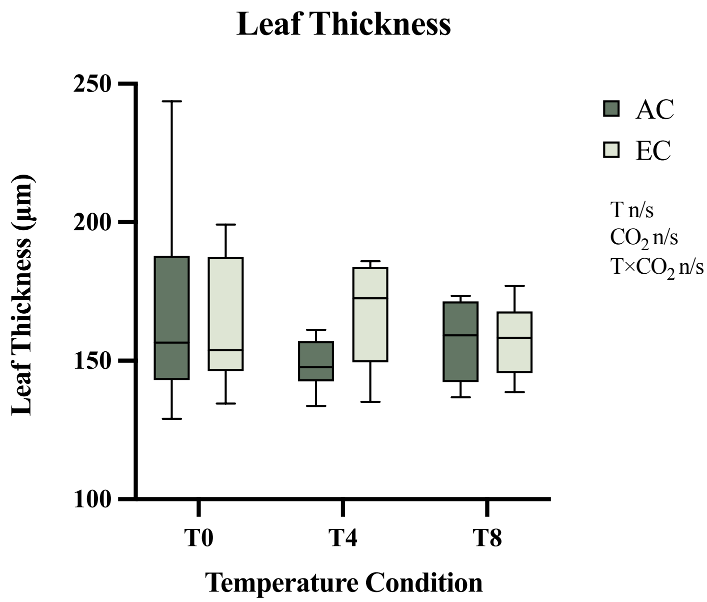

Figure 7. Mean (± SE) leaf thickness of *Betula papyrifera* at various climate conditions, where AC represents ambient atmospheric [CO_2] at 410 ppm, EC represents elevated atmospheric [CO_2] at 750 ppm, T0 represents ambient temperature, T4 represents +4°C warming, and T8 represents +8°C warming.

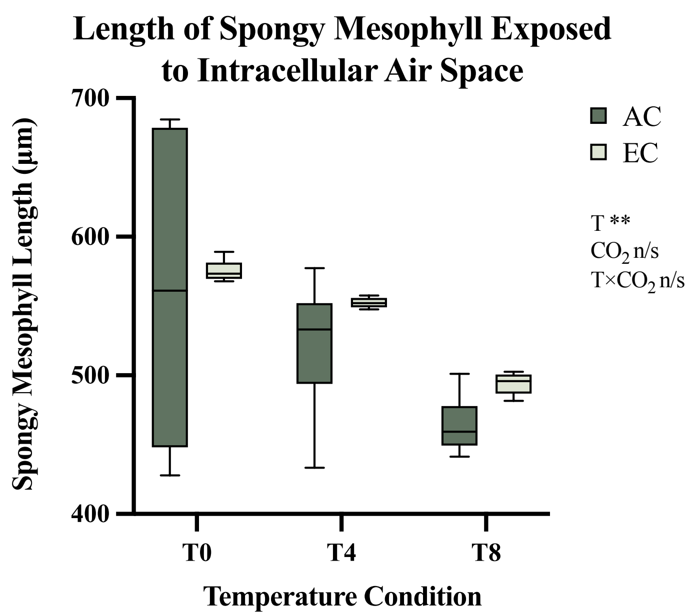

Figure 8. Mean (± SE) length of spongy mesophyll exposed to intracellular airspace of *Betula papyrifera* at various climate conditions, where AC represents ambient atmospheric [CO_2] at 410 ppm, EC represents elevated atmospheric [CO_2] at 750 ppm, T0 represents ambient temperature, T4 represents +4°C warming, and T8 represents +8°C warming.

Table 1. Summary of climatic conditions used to simulate current, moderate, and extreme climatic scenarios.

$[CO_2]$ conditions	Temperature Conditions		
Ambient $[CO_2]$ (AC): 410 ppm	Ambient Temperature (T0)	+4°C (T4)	+8°C (T8)
Elevated $[CO_2]$ (EC): 750 ppm	Ambient Temperature (T0)	+4°C (T4)	+8°C (T8)

Table 2. Raw data for stomatal density measurements, where stomatal density = number of stomata/unit area, and area = 2500 μm^2.

Sample #	CO_2 Condition	Temperature Condition	# of Stomata	Stomatal Density
1	AC	T0	377	0.151
2	AC	T0	420	0.168
3	AC	T0	423	0.169
4	AC	T0	427	0.171
5	AC	T0	430	0.172
6	AC	T0	422	0.169
1	AC	T4	440	0.176
2	AC	T4	438	0.175
3	AC	T4	452	0.181
4	AC	T4	461	0.184
5	AC	T4	468	0.187
6	AC	T4	444	0.178
1	AC	T8	470	0.188
2	AC	T8	460	0.184
3	AC	T8	481	0.192
4	AC	T8	478	0.191
5	AC	T8	480	0.192
6	AC	T8	482	0.193
1	EC	T0	343	0.137
2	EC	T0	323	0.129
3	EC	T0	306	0.122
4	EC	T0	324	0.130
5	EC	T0	347	0.139
6	EC	T0	311	0.124
1	EC	T4	420	0.168
2	EC	T4	383	0.153
3	EC	T4	425	0.170
4	EC	T4	422	0.169
5	EC	T4	426	0.170
6	EC	T4	431	0.172
1	EC	T8	471	0.188
2	EC	T8	468	0.187
3	EC	T8	470	0.188
4	EC	T8	472	0.189
5	EC	T8	467	0.187
6	EC	T8	474	0.190

Table 3. Raw data for stomatal size. Stomata were randomly sampled from a 2500 μm² which was previously defined to measure stomatal density.

			Length of Stomata										
Sample #	CO_2 Condition	Temperature Condition	1	2	3	4	5	6	7	8	9	10	Mean
1	AC	T0	36.387	40.024	56.123	39.120	39.823	37.146	42.265	34.003	42.352	41.441	**40.868**
2	AC	T0	45.048	36.297	43.228	46.646	39.283	41.202	41.576	38.478	39.224	30.543	**40.153**
3	AC	T0	39.811	33.848	48.048	32.509	38.929	39.987	42.759	34.483	39.409	31.160	**38.094**
4	AC	T0	37.259	31.614	43.758	39.246	36.745	43.732	39.853	32.148	32.822	42.551	**37.973**
5	AC	T0	40.796	40.914	46.984	30.904	38.102	41.271	31.622	40.180	33.650	46.493	**39.092**
6	AC	T0	44.477	32.771	39.958	38.594	36.700	46.626	41.182	35.600	42.491	40.255	**39.865**
1	AC	T4	36.658	33.918	30.741	36.360	36.709	38.785	26.772	34.209	27.663	30.927	**33.274**
2	AC	T4	35.310	35.679	32.492	33.910	29.154	29.902	32.822	38.247	31.404	43.778	**34.270**
3	AC	T4	34.019	33.161	33.357	35.177	33.427	35.128	32.650	35.414	28.229	31.829	**33.239**
4	AC	T4	32.795	30.255	34.690	38.649	36.276	29.682	29.849	34.033	35.760	45.193	**34.718**
5	AC	T4	39.163	34.033	37.390	32.386	38.792	29.085	35.592	35.136	35.715	33.611	**35.090**
6	AC	T4	33.883	34.810	36.861	44.697	39.046	41.322	40.193	32.537	35.117	42.426	**38.089**
1	AC	T8	33.179	29.506	33.787	34.675	32.132	32.877	30.317	35.744	33.159	31.817	**32.719**
2	AC	T8	34.359	31.220	34.252	31.266	32.376	33.994	29.536	31.264	34.416	34.825	**32.751**
3	AC	T8	37.292	40.148	32.226	33.161	29.317	31.243	30.821	41.163	30.220	36.489	**34.208**
4	AC	T8	30.063	36.893	35.621	31.890	35.050	34.340	36.586	33.786	29.849	32.986	**33.706**
5	AC	T8	30.440	28.831	29.138	33.894	34.033	36.543	28.976	33.017	31.205	34.696	**32.077**
6	AC	T8	29.531	31.539	33.537	34.324	27.567	32.826	31.755	35.184	34.870	24.593	**31.573**
1	EC	T0	37.134	39.835	45.689	44.450	46.022	48.917	47.441	45.332	47.949	44.976	**44.775**
2	EC	T0	39.835	46.624	38.499	39.739	40.105	42.811	41.463	45.843	42.759	42.322	**42.000**
3	EC	T0	45.431	39.234	38.574	41.699	36.189	38.204	37.774	37.791	33.898	39.685	**38.848**
4	EC	T0	40.750	40.193	35.760	36.521	34.217	34.095	38.253	35.347	37.645	32.315	**36.510**
5	EC	T0	35.925	44.264	39.929	36.067	41.917	38.543	37.967	32.266	34.990	37.073	**37.894**
6	EC	T0	38.366	35.943	39.260	36.960	37.561	39.546	38.253	40.346	35.950	37.718	**37.990**
1	EC	T4	37.373	46.298	46.583	44.680	41.262	37.547	36.543	41.411	42.014	39.014	**41.273**
2	EC	T4	31.606	43.533	40.063	36.936	43.695	41.158	36.604	33.790	36.356	39.046	**38.279**
3	EC	T4	39.758	38.594	40.773	39.026	33.017	39.240	31.205	36.700	37.589	36.700	**37.260**
4	EC	T4	33.537	34.825	37.547	34.825	37.098	37.366	34.217	34.171	35.950	33.427	**35.296**
5	EC	T4	34.825	36.313	33.925	35.184	37.267	41.157	34.095	34.810	33.427	35.303	**35.631**
6	EC	T4	35.848	38.851	37.547	39.200	38.905	35.362	38.225	39.974	37.561	34.990	**37.646**
1	EC	T8	32.376	30.714	31.539	31.138	34.416	42.756	29.690	33.017	27.261	32.778	**32.569**
2	EC	T8	32.778	36.914	29.849	28.685	30.440	27.319	26.102	34.825	32.132	27.567	**30.661**
3	EC	T8	31.406	33.801	34.033	35.303	36.197	43.773	28.849	38.005	30.388	38.594	**35.035**
4	EC	T8	32.969	38.965	33.005	30.137	34.056	36.244	31.539	33.088	35.778	28.197	**33.398**
5	EC	T8	39.100	33.195	34.340	30.990	34.708	36.262	37.991	28.566	42.549	34.033	**35.173**
6	EC	T8	31.323	29.549	29.095	32.376	25.840	27.049	29.120	32.067	32.650	32.539	**30.161**

Table 4. Raw data for palisade layer length.

			Palisade Layer Length										
Sample #	CO_2 Condition	Temperature Condition	1	2	3	4	5	6	7	8	9	10	Mean
1	AC	T0	42.948	43.813	46.706	45.547	47.095	63.348	66.695	43.121	49.781	49.277	**49.833**
2	AC	T0	47.953	55.157	60.049	73.128	86.598	45.358	49.470	46.081	53.953	49.535	**56.728**
3	AC	T0	66.310	71.177	64.086	57.988	55.546	55.329	57.669	70.245	48.382	67.755	**61.449**
4	AC	T0	71.792	68.339	64.389	74.355	60.962	66.108	68.394	60.276	51.869	66.307	**65.279**
5	AC	T0	51.649	64.146	51.431	46.941	55.828	48.294	67.043	63.834	103.267	118.055	**67.049**
6	AC	T0	48.696	49.430	47.291	143.730	162.715	75.057	61.743	57.109	58.218	59.485	**76.347**
1	AC	T4	46.693	42.386	50.702	46.141	53.395	66.809	49.705	47.328	71.498	55.402	**53.006**
2	AC	T4	60.258	65.406	63.807	62.587	55.752	75.743	61.391	59.527	63.587	60.018	**62.808**
3	AC	T4	72.389	66.085	55.015	64.141	60.439	74.127	54.943	53.083	54.013	69.065	**62.330**
4	AC	T4	58.359	53.772	50.224	59.559	50.214	53.853	61.133	67.713	55.543	56.526	**56.690**
5	AC	T4	53.209	52.689	49.657	37.912	43.176	59.586	62.120	57.342	52.927	54.160	**52.278**
6	AC	T4	42.537	38.430	41.995	50.805	50.697	50.177	50.541	50.326	64.958	53.652	**49.412**
1	AC	T8	40.324	48.447	48.122	37.098	45.002	45.358	42.058	42.405	45.132	40.654	**43.460**
2	AC	T8	53.309	45.614	40.750	50.954	38.902	43.012	41.565	39.659	46.476	46.024	**44.627**
3	AC	T8	45.266	59.160	38.250	47.760	66.236	42.439	114.188	96.561	88.570	84.199	**68.263**
4	AC	T8	53.121	47.328	62.295	47.488	53.523	38.233	66.115	67.438	68.424	71.313	**57.528**
5	AC	T8	59.285	50.440	47.499	58.858	66.241	46.895	45.969	41.082	61.908	51.299	**52.948**
6	AC	T8	59.957	46.940	44.759	46.146	46.703	46.016	48.582	65.824	54.997	65.701	**52.563**
1	EC	T0	47.128	50.856	52.497	47.251	46.888	50.964	51.578	48.211	47.177	51.151	**49.370**
2	EC	T0	50.044	43.061	51.717	41.792	52.624	47.055	51.350	52.401	45.480	40.852	**47.638**
3	EC	T0	37.647	47.959	44.102	70.341	68.364	68.748	41.984	31.636	60.002	64.206	**53.499**
4	EC	T0	36.594	37.066	37.746	57.878	63.428	59.258	61.374	36.572	45.884	57.195	**49.300**
5	EC	T0	60.275	54.107	65.407	62.517	72.388	71.163	58.382	56.158	54.709	57.413	**61.252**
6	EC	T0	51.787	54.892	50.989	56.391	61.943	61.390	63.964	60.318	62.377	62.253	**58.630**
1	EC	T4	67.331	71.127	64.467	63.492	31.901	64.561	57.565	72.892	74.196	54.262	**62.179**
2	EC	T4	56.660	47.862	69.777	76.956	64.972	72.403	77.480	80.330	72.221	68.098	**68.676**
3	EC	T4	46.586	43.515	52.214	49.620	54.891	46.071	62.587	53.248	54.887	57.081	**52.070**
4	EC	T4	47.977	50.177	60.015	59.735	54.638	52.878	60.209	58.478	51.708	47.855	**54.367**
5	EC	T4	79.819	75.950	77.961	70.446	69.500	75.812	81.246	79.969	79.744	81.515	**77.196**
6	EC	T4	67.728	71.162	70.279	90.563	66.400	78.189	79.962	86.331	108.762	85.512	**80.489**
1	EC	T8	68.214	62.244	63.480	54.786	59.910	70.763	63.967	58.236	58.848	56.269	**61.672**
2	EC	T8	58.213	61.811	70.272	64.970	65.412	62.802	57.545	69.869	58.702	58.759	**62.836**
3	EC	T8	68.560	47.503	66.980	66.824	52.608	58.141	68.645	51.735	69.634	59.996	**61.063**
4	EC	T8	66.780	62.235	57.020	50.797	57.306	67.362	49.164	49.525	49.230	53.055	**56.247**
5	EC	T8	82.878	70.909	70.673	68.832	69.807	81.443	78.800	68.630	76.786	84.192	**75.295**
6	EC	T8	66.390	70.761	77.683	73.872	82.487	82.232	91.442	80.701	74.817	83.897	**78.428**

Table 5. Raw data for leaf thickness.

			Leaf Thickness										
Sample #	CO_2 Condition	Temperature Condition	1	2	3	4	5	6	7	8	9	10	Mean
1	AC	T0	132.546	152.538	162.759	123.337	163.780	168.660	163.472	165.472	167.007	145.385	**154.496**
2	AC	T0	329.211	143.860	123.702	152.089	162.607	151.150	139.349	115.980	128.864	138.501	**158.531**
3	AC	T0	145.401	125.795	144.449	139.773	165.731	161.566	175.520	136.788	147.992	134.746	**147.776**
4	AC	T0	136.392	158.296	142.777	137.530	112.857	146.971	113.930	117.349	118.078	106.309	**129.049**
5	AC	T0	158.313	178.704	146.515	137.058	139.639	130.311	126.094	250.702	154.120	271.644	**169.310**
6	AC	T0	495.721	437.416	397.253	165.633	165.800	159.365	135.339	163.538	163.235	153.415	**243.672**
1	AC	T4	125.357	113.851	124.724	147.432	155.250	140.263	129.091	131.084	142.077	127.139	**133.627**
2	AC	T4	134.836	147.443	135.485	139.243	164.884	144.386	152.107	142.398	156.415	149.973	**146.717**
3	AC	T4	160.006	176.345	127.751	162.837	153.401	175.371	152.617	172.913	159.370	171.270	**161.188**
4	AC	T4	151.195	160.630	157.720	168.310	134.225	159.744	157.097	130.040	172.903	165.364	**155.723**
5	AC	T4	154.267	132.405	165.084	126.387	174.348	156.232	146.419	129.260	143.249	157.720	**148.537**
6	AC	T4	134.041	134.789	124.169	135.147	183.064	123.796	129.059	134.634	208.053	148.806	**145.556**
1	AC	T8	138.889	137.863	150.973	144.589	128.565	137.274	115.814	145.424	124.088	144.571	**136.805**
2	AC	T8	124.354	147.981	137.366	128.267	120.225	154.779	148.133	166.297	144.732	169.015	**144.115**
3	AC	T8	169.342	130.562	135.447	121.840	111.514	209.637	205.418	206.418	157.420	158.701	**160.630**
4	AC	T8	146.035	139.783	148.514	155.215	145.059	157.902	160.578	196.108	173.148	155.806	**157.815**
5	AC	T8	183.546	167.280	160.111	172.889	149.614	185.717	181.760	171.193	170.316	164.713	**170.714**
6	AC	T8	167.758	166.344	162.859	199.568	215.982	236.750	158.744	158.153	136.497	131.722	**173.438**
1	EC	T0	160.480	191.953	192.518	125.120	133.599	142.447	136.397	128.626	148.254	142.904	**150.230**
2	EC	T0	149.300	156.117	125.439	132.209	147.123	138.113	126.517	129.238	130.639	111.401	**134.610**
3	EC	T0	183.877	192.259	133.633	158.912	111.226	188.183	171.220	134.953	141.366	108.596	**152.423**
4	EC	T0	187.515	170.983	185.553	122.740	117.689	177.530	185.850	150.807	144.783	107.410	**155.086**
5	EC	T0	226.325	173.508	316.215	173.045	173.368	160.695	177.114	150.497	140.022	144.311	**183.510**
6	EC	T0	149.639	177.614	162.859	150.618	400.173	297.375	178.064	149.949	159.801	165.412	**199.150**
1	EC	T4	135. 190	217.340	185.335	169.950	150.754	173.096	169.872	180.902	156.325	164.786	**174.262**
2	EC	T4	192.773	206.609	203.741	156.747	158.320	199.220	226.734	190.893	149.297	146.592	**183.093**
3	EC	T4	154.595	146.405	160.699	176.098	152.555	174.863	145.389	147.517	140.277	144.154	**154.255**
4	EC	T4	110.757	100.961	153.626	119.918	165.243	126.599	135.392	181.888	114.165	143.136	**135.169**
5	EC	T4	155.407	170.396	150.650	179.450	170.556	181.399	216.235	144.913	139.427	199.892	**170.833**
6	EC	T4	172.186	197.657	175.362	193.682	175.478	193.359	181.168	202.095	186.800	181.841	**185.963**
1	EC	T8	119.574	122.613	127.235	159.791	157.229	185.040	175.991	124.552	161.316	144.902	**147.824**
2	EC	T8	221.155	136.505	141.182	111.374	113.880	127.751	113.564	161.776	126.969	133.104	**138.726**
3	EC	T8	150.808	156.117	133.962	134.667	167.082	184.585	146.461	166.185	163.884	140.768	**154.452**
4	EC	T8	203.694	163.763	133.281	182.035	194.951	181.921	134.146	183.373	139.543	130.303	**164.701**
5	EC	T8	169.090	173.855	163.826	162.228	178.498	125.895	151.080	144.517	203.800	149.833	**162.262**
6	EC	T8	206.152	165.141	168.132	144.154	187.723	174.376	186.502	171.034	195.815	171.371	**177.040**

Table 6. Raw data for spongy mesophyll cell length exposed to intracellular air space. Measurements were taken within a defined 100 µm wide section of the leaf.

			Length of Spongy Mesophyll Exposed to Intracellular Space										
Sample #	CO_2 Condition	Temperature Condition	1	2	3	4	5	6	7	8	9	10	Mean
1	AC	T0	678.054	570.720	1028.358	1231.068	550.016	513.636	527.874	724.991	542.403	478.093	**684.521**
2	AC	T0	302.427	468.294	388.606	796.050	636.080	426.861	312.240	353.990	476.870	386.284	**454.770**
3	AC	T0	335.704	405.076	502.225	413.558	523.698	407.706	679.830	327.264	567.691	596.523	**475.928**
4	AC	T0	544.646	364.496	451.883	389.435	413.665	411.703	515.918	351.438	415.878	418.933	**427.800**
5	AC	T0	552.718	401.301	699.254	670.614	862.712	644.555	789.737	1056.358	565.287	524.894	**676.743**
6	AC	T0	1492.153	921.583	557.988	478.974	455.790	685.721	379.666	487.543	612.899	390.443	**646.276**
1	AC	T4	392.461	580.292	482.891	578.163	508.133	470.962	641.194	520.397	456.380	610.790	**524.166**
2	AC	T4	470.647	384.226	349.672	529.259	379.396	529.274	449.863	486.041	366.180	388.022	**433.258**
3	AC	T4	873.543	610.736	568.204	512.678	391.971	426.348	629.241	654.396	569.760	537.476	**577.435**
4	AC	T4	430.487	512.067	384.247	632.639	578.845	489.234	438.403	476.920	617.898	579.738	**514.048**
5	AC	T4	518.263	477.819	530.384	478.712	645.469	516.926	535.047	461.888	634.765	620.649	**541.992**
6	AC	T4	324.859	576.840	629.800	856.739	490.840	550.394	578.394	623.483	370.489	434.380	**543.622**
1	AC	T8	283.517	428.220	389.395	509.747	511.945	402.014	496.385	463.576	632.363	583.913	**470.108**
2	AC	T8	367.044	442.454	512.760	453.275	399.278	378.275	410.547	528.489	453.420	592.222	**453.776**
3	AC	T8	403.898	542.331	608.138	649.890	407.465	298.794	567.803	657.858	518.443	356.246	**501.087**
4	AC	T8	436.058	460.624	489.537	445.631	658.297	319.804	289.808	335.794	503.793	582.083	**452.143**
5	AC	T8	368.794	456.290	620.803	563.858	290.734	367.893	530.683	469.278	471.678	274.667	**441.468**
6	AC	T8	448.892	421.982	531.015	572.826	623.794	298.823	376.792	513.445	410.676	450.333	**464.858**
1	EC	T0	569.595	635.284	801.816	756.294	469.204	397.205	389.560	473.689	719.195	680.348	**589.219**
2	EC	T0	893.025	710.740	613.470	523.284	623.734	395.123	328.480	564.074	590.129	484.705	**572.676**
3	EC	T0	513.659	682.139	756.534	638.938	550.704	438.972	456.310	513.760	539.776	612.348	**570.314**
4	EC	T0	674.565	532.606	542.642	667.407	439.686	479.157	529.365	617.486	604.417	699.772	**578.710**
5	EC	T0	649.228	455.134	528.556	801.833	465.265	530.754	579.058	550.213	686.251	433.635	**567.993**
6	EC	T0	543.793	681.723	592.467	478.716	427.614	569.031	597.927	652.095	547.881	647.818	**573.907**
1	EC	T4	429.662	519.843	839.644	327.465	489.007	548.330	602.894	610.547	546.790	561.398	**547.558**
2	EC	T4	730.385	609.699	556.900	432.763	450.891	598.049	377.812	573.244	609.172	578.194	**551.711**
3	EC	T4	572.397	516.112	513.820	558.335	670.042	408.236	589.238	561.468	631.522	554.094	**557.526**
4	EC	T4	670.042	801.009	347.870	548.171	479.855	524.950	482.622	552.341	621.229	468.222	**549.631**
5	EC	T4	538.626	515.609	583.219	551.813	716.056	730.776	472.499	394.333	443.432	578.284	**552.465**
6	EC	T4	552.389	476.337	527.439	622.222	394.488	707.446	538.120	618.007	529.440	586.012	**555.190**
1	EC	T8	356.199	378.360	435.229	516.387	589.338	472.008	486.990	527.235	531.264	593.988	**488.700**
2	EC	T8	358.460	467.165	545.392	398.778	545.554	587.304	531.873	436.512	553.210	530.400	**495.465**
3	EC	T8	431.996	473.947	567.446	589.727	507.113	406.795	390.046	552.216	495.653	548.551	**496.349**
4	EC	T8	508.827	550.967	390.046	532.140	459.065	545.190	490.311	398.421	457.583	483.468	**481.602**
5	EC	T8	433.094	503.992	494.649	511.693	521.633	588.919	526.709	532.954	518.514	367.280	**499.944**
6	EC	T8	513.488	537.637	390.145	343.849	402.536	517.281	572.129	653.173	620.347	476.618	**502.720**